Validity of the *SD*-pair truncation of the shell model

Y. M. Zhao,[1,4] N. Yoshinaga,[2] S. Yamaji,[1] and A. Arima[3]
[1]*Cyclotron Laboratory, Institute of Physical and Chemical Research (RIKEN), Hirosawa 2-1, Wako-shi, Saitama, 351-0198, Japan*
[2]*Department of Physics, Saitama University, Urawa, Saitama, 338-0825, Japan*
[3]*The House of Councilors, 2-1-1 Nagatacho, Chiyodaku, Tokyo, 100-8962, Japan*
[4]*Department of Physics, Southeast University, Nanjing 210018, People's Republic of China*
(Received 21 December 1999; published 22 June 2000)

The validity of the *SD*-pair truncation of the shell model is tested in a single *j* shell and in many *j* shells within the framework of the nucleon pair shell model. It is found that the *SD*-pair truncation is a good approximation of the shell model in the single-*j* case when the Hamiltonian consists of (monopole and quadrupole) pairing plus quadrupole-quadrupole-type interaction. The *SD*-pair truncation deteriorates if the quadrupole-quadrupole interaction is artificially large compared with the monopole pairing interaction. For multi-*j* shells, schematic calculations in the degenerate *sd*, *pf*, and *sdg* shells are performed for the extreme case of a pure quadrupole-quadrupole interaction. There is a large difference between the binding energies in the *SD*-pair-truncated subspace and those calculated in the full shell model space as in the case of a single-*j* shell. However, it is found that the basic properties of the band structure remain intact, and that the difference in energy levels, i.e., moments of inertia, can be easily absorbed by adjusting interaction strengths without changing the transition rates.

PACS number(s): 21.10.Re, 21.60.Cs, 21.60.Ev, 23.20.Js

I. INTRODUCTION

The interacting boson model (IBM) [1] has proved to be a great success in describing the low-lying nuclear collective motion in medium and heavy mass nuclei. Since the invention of the IBM, many efforts have been made to understand the microscopic foundation of the IBM. In the IBM, the Hamiltonian and the configuration space are constructed using *s* and *d* bosons. These bosons are interpreted as coherent *SD* nucleon pairs with angular momenta of 0 and 2, respectively. Therefore, in order to derive the IBM Hamiltonian from the shell model, one first needs to check the validity of nucleon pair approximation of the shell model. It is very interesting to study how well the diagonalization of the Hamiltonian in the *SD*-pair-truncated subspace, which are determined to maximize the nuclear collectivity, can reproduce the results of full shell model (SM).

Recently, the authors of Ref. [2] generalized the Wick theorem, which works efficiently for coupled fermion pairs. Based on this technique, they proposed a nucleon-pair shell model (NPSM) [3]. In the NPSM, nucleon pairs with various angular momenta are used as the building blocks of the truncated shell model space. If these building blocks are restricted to *SD* pairs, the NPSM is reduced to the SD pair approximation of the shell model. Using an ordinary personal computer, one can calculate up to four or even five proton and neutron pairs outside the inert core for multi-*j* shells. In this paper, we test the *SD*-pair approximation for both a single closed shell and an open shell by comparing the calculated results in the *SD*-pair subspace and results in the full SM space. If calculated results of low-lying states are very consistent with or close to the results in the full SM space, the *SD*-pair truncation is said to be a good approximation of the SM.

Prior to this work, many papers (e.g., Ref. [4]) tested (the *SD*-pair truncation of the shell model space. The difference in this paper is that we go to open shells for multi-*j* cases of up to three pairs. In previous studies, comparisons of calculations within the *SD*-pair subspace and the shell model space were presented only for up to three pairs for the two-*j* case of a single closed shell, or two proton pairs and two neutron pairs of open shells. The multi-*j* case was rather difficult to tackle in the past. One of the reasons for this is that without the technique of Ref. [2] it would be very difficult to calculate the matrix elements in the *SD*-pair configurations when the *D* pair number is equal to or greater than 3. In this paper, we present a comparison between the *SD*-pair approximation and the full shell model calculation throughout the whole schematic single-*j* ($nlj=55\frac{11}{2}$) shell, where we assume a residual interaction of pairing plus a quadrupole-quadrupole interaction which simulates vibrational nuclei. In the degenerate *sd*, *pf*, and *sdg* shells, we assume that the Hamiltonian consists of pure quadrupole-quadrupole interaction since this is the case where Elliott's SU(3) model is applied, and exact results are known analytically. Here it is expected that the *SD*-pair approximation is rather poor, since earlier works indicated that we need higher angular momentum pairs such as *G* pairs [4]. In this paper, however, we show that essential properties such as band structures are kept intact within the *SD* subspace, and that the difference in moment of inertia can be absorbed by adjusting interaction strength.

This paper is organized as follows. In Sec. II, we specify our definition of *S* and *D* pairs and the Hamiltonian. In Sec. III, we study a doubly even proton-neutron system which is a single-*j* shell using the (monopole and quadrupole) pairing plus *QQ* interaction. In Sec. IV, we study degenerate *sd*, *pf*, and *sdg* shells assuming pure a quadrupole-quadrupole interaction in the Hamiltonian. Then we compare the results of the *SD*-pair truncation with analytical results of Elliott's SU(3) model. Discussions and a conclusion are given in Sec. V.

II. *SD*-PAIR APPROXIMATION AND THE HAMILTONIAN

The collective pair of angular momentum r, with its projection μ, is defined as

$$A^{r\dagger}_{\mu}=\sum_{ab} y(abr)(C^{\dagger}_{a}\times C^{\dagger}_{b})^{r}_{\mu}, \tag{1}$$

where $C^{\dagger}_{a}$ and $C^{\dagger}_{b}$ are single-particle creation operators, and $r=0$ and 2 correspond to the *SD* pairs, respectively. a and b denote all quantum numbers (except the magnetic quantum number) necessary to specify a state $[a\equiv(nlj)]$. We also use them to denote the angular momentum of the single-particle orbit, where there is no confusion (i.e., a is used to label the single-particle orbit as well as to denote the corresponding j value). $y(abr)$ are structure coefficients of the collective pairs. These *SD* pairs are coupled step by step to yield a complete set of the N *SD*-pair subspace, which has the same dimension as the sd IBM boson space in general except for few cases where some states are Pauli forbidden.

In this paper, the Hamiltonian is chosen as

$$H=H_{\pi}+H_{\nu}+\kappa Q_{\pi}Q_{\nu}. \tag{2}$$

The above H_{π} and H_{ν} are Hamiltonians for valence protons and valence neutrons, respectively, which consist of single-particle energy, monopole and quadrupole pairing, and quadrupole quadrupole particle-hole interaction. Their explicit forms are

$$H_{\sigma}=\sum_{\alpha}\epsilon_{\alpha\sigma}C^{\dagger}_{\alpha\sigma}C_{\alpha\sigma}+G_{\sigma}\mathcal{P}^{\dagger}_{\sigma}\mathcal{P}_{\sigma}+G^{2}_{\sigma}\mathcal{P}^{(2)\dagger}_{\sigma}\mathcal{P}^{(2)}_{\sigma}+\kappa_{\sigma}Q_{\sigma}Q_{\sigma}, \tag{3}$$

where σ stands for π or ν, and

$$\mathcal{P}^{\dagger}_{\sigma}=\frac{\hat{j}_{\sigma}}{2}(C^{\dagger}_{a\sigma}C^{\dagger}_{a\sigma})^{0}_{0},$$

$$\mathcal{P}^{(2)\dagger}_{\sigma M}=\sum_{a_{\sigma}b_{\sigma}} q(a_{\sigma}b_{\sigma})(C^{\dagger}_{a\sigma}\times C^{\dagger}_{b\sigma})^{2}_{M}, \tag{4}$$

with $\hat{j}_{\sigma}=(2j_{\sigma}+1)^{1/2}$, and $M=0,\pm1,\pm2$; $q(a_{\sigma}b_{\sigma})$ is the same factor as that which appears in the Q_{σ} operator, which is defined as

$$Q_{\sigma M}=\sum_{a_{\sigma}b_{\sigma}} q(a_{\sigma}b_{\sigma})(C^{\dagger}_{a\sigma}\times\tilde{C}_{b\sigma})^{2}_{M}$$

$$=-\sum_{a_{\sigma}b_{\sigma}}\frac{1}{\sqrt{5}}\langle a_{\sigma}\|r^{2}Y^{2}\|b_{\sigma}\rangle(C^{\dagger}_{a\sigma}\times\tilde{C}_{b\sigma})^{2}_{M}. \tag{5}$$

It is easy to show that

$$q(ab)=\frac{(-)^{j+1/2}}{\sqrt{20\pi}}\hat{j}\hat{j}'C^{20}_{j1/2,j'-1/2}\langle nl|r^{2}|nl'\rangle,$$

where $C^{20}_{j1/2,j'-1/2}$ is the Clebsch-Gordan coefficient. The matrix elements for r^2 are given in [5]:

TABLE I. Parameters used in the Hamiltonian. G_{σ} is in MeV, and G^{2}_{σ}, κ_{σ}, and κ are in MeV/fm^4. $G^{2}_{\pi}=G^{2}_{\nu}$ and $\kappa_{\pi}=\kappa_{\nu}$ for simplicity. The sign of κ is negative if the valence shells of both protons and neutrons are half-filled before or half-filled afterward; otherwise it is positive.

G_{ν}	G_{π}	G^{2}_{σ}	κ_{σ}	κ
-0.131	-0.180	-0.023	-0.020	±0.07

$$\langle nl|r^{2}|nl'\rangle=\begin{cases}(n+3/2)r^{2}_{0}, & l=l',\\ (n+l'+2\pm1)^{1/2}(n-l'+1\mp1)^{1/2}r^{2}_{0}, & l=l'\pm2,\end{cases} \tag{6}$$

where $r^{2}_{0}=\hbar/M_{N}\omega_{0}=1.012A^{1/3}$ fm^2, and the harmonic-oscillator wave function is used. M_N is nucleon mass and ω_0 is the harmonic-oscillator frequency. In this paper, we fix $r_0\equiv1$ fm for the sake of simplicity.

III. SINGLE-*j* CASE

The single-j shell is the simplest case because one has only one kind of S pair and D pair, i.e., $y(abr)=\delta_{aj}\delta_{bj}$. Here we choose $(nlj)=(55\frac{11}{2})$, with $\epsilon_{11/2}=0$. One set of Hamiltonian parameters, which simulates vibrational nuclei, is listed in Table I. Figure 1 presents a detailed comparison

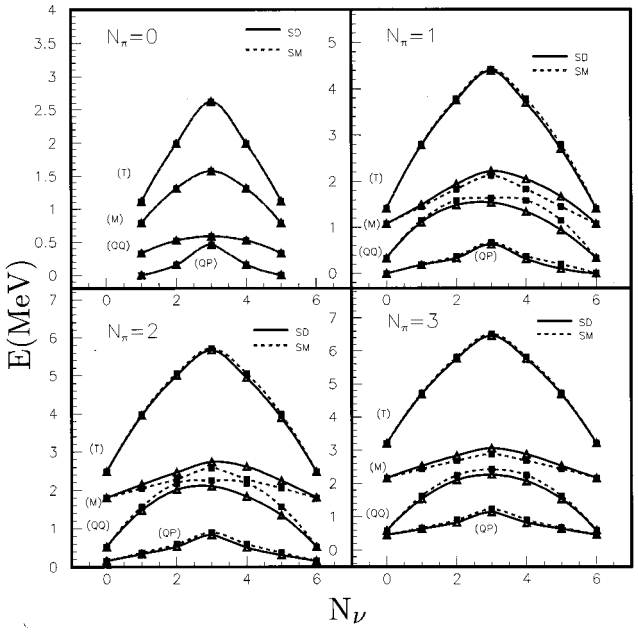

FIG. 1. Total binding energies T and contribution to binding energies (in MeV) from the monopole pairing term M, quadrupole pairing term (QP), and quadrupole-quadrupole (QQ) interactions for the single-j case. The abscissa is N_{ν}, and the ordinate is the binding energy (or the contribution to the binding energy). N_{π} and N_{ν} are numbers of proton and neutron pairs, respectively. The dotted lines are results calculated in the full shell model space, and the solid lines are results calculated using the *SD*-pair truncation.

of calculated binding energy from each term within the *SD*-pair subspace and that in the whole SM space. Note that the single-particle contribution is omitted, since this term is not interesting in a single-*j* shell. The total binding energies are almost perfectly reproduced. It is easy to notice from Fig. 1 that among the contributions to binding energies from all terms in the Hamiltonian the quadrupole pairing contribution within the *SD*-pair subspace agrees well with that within the whole SM space. In the open shell, the contribution from monopole pairing interaction calculated in the SM space is slightly and systematically smaller than that from the corresponding term using the *SD*-pair truncation. On the other hand, contributions from the quadrupole-quadrupole interaction and the quadrupole pairing interaction using the *SD*-pair truncation are systematically smaller than those from the corresponding terms in the SM space. Because the above two opposite disagreements cancel each other out, the total binding energy calculated in the shell model space and that calculated in the *SD*-pair truncation are almost the same in magnitude [6].

According to the above calculation, it is expected that if the strength κ is gradually enlarged the agreement of binding energy between these two calculations deteriorate because the contribution to binding energy from quadrupole-quadrupole interaction which is calculated in the full shell model space is larger than that calculated in the *SD*-pair truncation. On the other hand, however, because the ground state in the *SD*-pair truncation can never be lower than that in the SM calculation, and the contribution to binding energy from monopole pairing in the *SD*-pair truncation is larger than its contribution calculated in the SM calculation, we expect that the agreement between calculated binding energies in the *SD* subspace and those calculated in the full shell model space should not deteriorate if we artificially increase the pairing interaction strength. We note that in the single closed (i.e., $N_\pi=0$, here N_π means number of proton pairs) case, the contribution of binding energies from every term is exactly the same as that from the shell model calculation. In fact, for the single closed shell of $j=11/2$, the dimension of 0^+ states in the *SD*-pair subspace is always the same as that in the shell model space. As a consequence, the calculation of *every* term in the *SD*-pair subspace *must* be equivalent to that in the shell model space. The eigenvalues and wave functions for all the 0^+ states in the *SD*-pair subspace are *identical* as those in the shell model. In the case of an open shell, the situation is different, since the dimension of the shell model space is much larger than that of the *SD*-pair subspace. From Fig. 1, it is also easy to notice that when the nucleon pair number is more than $1/2\Omega_j=1/2(j+1/2)=3$ and $N_\pi=1$ or 2, the agreement between the term by term contribution calculated in the *SD*-pair truncation and that calculated in the full SM space is not satisfactory, especially for the contribution from monopole pairing and quadrupole-quadrupole force. The differences of these two terms, which are comparable in magnitude and opposite in sign, are quite large. An unexpected phenomenon is that the above differences become very small for the cases of $N_\pi=3$ or $N_\nu=3$. This behavior of the half-filled case is even more surprising in the schematic multi-*j* case in Sec. IV. In Fig. 2, we present

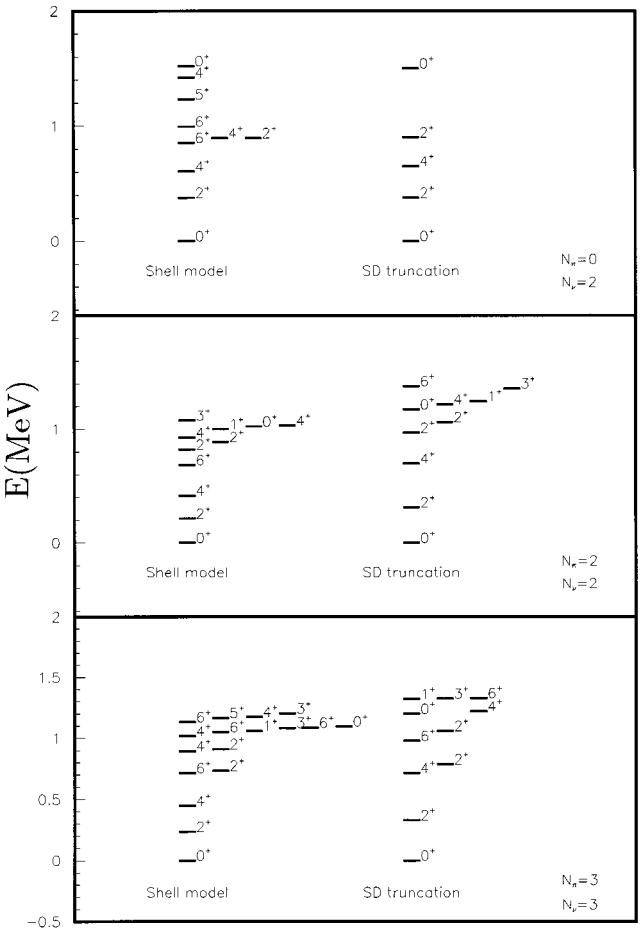

FIG. 2. Excitation energies (in MeV) in the single-*j* case. The left-hand side presents the results calculated in the full shell model space, and the right-hand side gives results in the truncated *SD*-pair subspace. Refer to Table I for the parameters.

a comparison between low-lying excited energies which are calculated in the *SD*-pair subspace and those calculated in the full SM space for three typical cases. The other cases are omitted to save space in this paper. Although the configuration space of the shell model is much larger than that of its *SD*-pair subspace, low-lying states, e.g., 2_1^+, 4_1^+, etc., are reasonably reproduced if they belong to the *SD*-pair subspace.

Some important $E2$ transitions between low-lying states in the *SD*-pair subspace are calculated using $e_\pi=1.3e$ and $e_\nu=0.9e$. A comparison between these $E2$ transition rates calculated in the *SD* subspace and those calculated in the shell model is given in Table II. According to Table II, $E2$ transitions between low-lying states such as $2_1^+\rightarrow 0_1^+$, $2_2^+\rightarrow 0_2^+$, $4_1^+\rightarrow 2_1^+$, and $2_2^+\rightarrow 2_1^+$ agree well in the two calculations (the SM and its *SD*-pair truncation). The calculated transitions of $4_2^+\rightarrow 2_1^+$ and $4_2^+\rightarrow 2_2^+$ in the *SD*-pair truncation sometimes do not fit well with results calculated in the full shell model space. The reason is that the 4_2^+ state in the shell model does not necessarily correspond to the 4_2^+ state in the *SD*-pair truncation (the energy density of the shell model is much larger than that of the *SD*-pair subspace in

TABLE II. Some typical $E2$ transition strengths (single-j case). We use $e_\pi = 1.3e$ and $e_\nu = 0.9e$. The $E2$ transition strengths are in e^2 fm^2.

N_ν	N_π	$2_1^+ \to 0_1^+$	$2_2^+ \to 0_2^+$	$2_2^+ \to 2_1^+$	$4_1^+ \to 2_1^+$	$4_2^+ \to 2_1^+$	$4_2^+ \to 2_2^+$
0	2(SM)	8.8452	2.2645	10.7132	10.2204	2.1271	1.0256
0	2(SD)	8.8449	2.6486	10.8173	6.5606	-	-
1	3(SM)	14.3868	0.0580	2.9370	22.9947	0.0459	10.0865
1	3(SD)	13.8129	0.0985	3.3962	16.5084	1.6374	2.6001
2	0(SM)	4.2304	1.0924	5.1663	5.0031	0.8968	0.5128
2	0(SD)	4.2301	1.2716	5.2178	3.1239	-	-
2	2(SM)	18.8828	3.8025	10.7182	27.4768	1.8276	1.4833
2	2(SD)	16.8025	4.5778	9.7368	19.8780	2.1620	0.5085
3	1(SM)	14.0455	1.3931	12.2893	19.2383	0.2273	5.5107
3	1(SD)	12.3957	1.5299	11.9986	13.6100	0.0000	3.4772
3	3(SM)	21.4689	8.5278	31.7663	30.1148	0.0000	16.5408
3	3(SD)	19.5008	7.0591	26.9541	23.4722	0.7646	12.1028

many cases). There is a possibility that 4_2^+ is related to the hexadecapole degree of freedom.

Although the agreement of higher states does not seem very good in cases of open shells, the results indicate that in this small single-j shell the SD-pair truncation is an extremely good approximation of the full shell model for the low-lying states, because the calculation within the SD-pair subspace reasonably reproduces most of the physical quantities. In other words, although the SD-pair subspace is much smaller than the full shell model space in the above calculations, it includes most important parts of the shell model space for low-lying excitations in the above single-j shell. We emphasize here that the good agreement in this case is partly due to the facts that we have a moderate pairing strength and that j is very small. In the case of deformed nuclei where quadrupole-quadrupole interaction is strong and the j value is large, the results might not be so good.

IV. MULTI-j CASES

Calculation in a multi-j shell is much more complicated and time consuming than that in a single-j shell, both for the SM calculation and its SD-pair approximation. In the SM calculation in a multi-j shell, up to 6–8 particles can be tackled in a single closed shell (depending on the degeneracy of the shell). In the realistic case of an open shell, it is extremely difficult or even impossible to carry out the shell model calculation when particle numbers of both valence protons and valence neutrons go up to 6 for medium and heavy nuclei, because the dimension of the configuration space is tremendously or even prohibitively huge.

Fortunately, for deformed nuclei one can apply Elliott's SU(3) model for the degenerate *sd*, *pf*, and *sdg* shells when the Hamiltonian is assumed to be pure quadrupole-quadrupole interaction. In this section, the Hamiltonian is chosen to be symmetric between protons and neutrons, and to be written in terms of the Casimir operators of the group chain $\mathrm{SU}(K) \supset \mathrm{SU}(3) \supset \mathrm{O}(3)$ ($K=6$, 10, and 15 for the *sd*, *pf*, and *sdg* shells, respectively [7]). H is written as

$$H = -\kappa(Q_\pi + Q_\nu)(Q_\pi + Q_\nu) = -\kappa \frac{5}{2\pi}\left(\frac{1}{2}(\lambda^2+\lambda\mu+\mu^2+3\lambda+3\mu) - \frac{3}{8}L(L+1)\right), \tag{7}$$

where $\frac{1}{2}(\lambda^2+\lambda\mu+\mu^2+3\lambda+3\mu) = C_{\mathrm{SU}(3)_{\pi\nu}}$ is the eigenvalue of the Casimir operator for the $\mathrm{SU}(3)_{\pi\nu}$ group, and κ is chosen to be $16\pi/5$(MeV) for the sake of simplicity. It should be noted that this Hamiltonian depends only on the orbital angular momentum, and is completely free from the spin degree of freedom. The single-particle levels are denoted by

$$(nlj) = (20_{\frac{1}{2}}),(22_{\frac{3}{2}}),(22_{\frac{5}{2}}) \quad \text{for the } sd \text{ shell,}$$
$$(nlj) = (31_{\frac{1}{2}}),(31_{\frac{3}{2}}),(33_{\frac{5}{2}}),(33_{\frac{7}{2}}) \quad \text{for the } pf \text{ shell,} \tag{8}$$
$$(nlj) = (40_{\frac{1}{2}}),(42_{\frac{3}{2}}),(42_{\frac{5}{2}}),(44_{\frac{7}{2}}),(44_{\frac{9}{2}}) \quad \text{for the } sdg \text{ shell.}$$

There are several tables [7] of irreducible representations for the $\mathrm{SU}(K) \supset \mathrm{SU}(3) \supset \mathrm{O}(3)$ for the *sd* and *sdg* shells. In Table III, we list several low-lying $\mathrm{SU}(3)_{\pi\nu}$ irreducible representations $(\lambda,\mu)^S_{\pi\nu} = (\lambda,\mu)^{S_\pi}_{\pi} \times (\lambda,\mu)^{S_\nu}_{\nu}$ which are interesting in our consideration. The suffix S represents the spin angular momentum.

Now we come to the question of the SD pair structures. First we solve the BCS equation to obtain u_a and v_a, the empty and occupied amplitudes for orbit a for a certain pairing interaction, respectively. Because we use the degenerate single-particle levels, these u_a and v_a are independent on the pairing strengths. The collective S pair is defined to be [8]

$$S^\dagger = \sum_a y(aa0)(C_a^\dagger \times C_a^\dagger)^0,$$

TABLE III. In this table, we list several $SU(3)_{\pi\nu}$ irreducible representations which correspond to the low-lying excitation bands. $(\lambda_\nu,\mu_\nu)^{S_\nu}$ and $(\lambda_\pi,\mu_\pi)^{S_\pi}$ and their direct products are sufficient to present (at least) low-lying bands, although they are incomplete (a complete table is too large). The superscripts S_π and S_ν are spins corresponding to irreducible representations of proton and neutron degrees of freedom, respectively. The total spin **S** is determined using $\mathbf{S}=\mathbf{S}_\pi+\mathbf{S}_\nu$. The case $S=0$ corresponds to $S_\pi=S_\nu=0$; $S=1$ corresponds to $S_\pi(S_\nu)=0(1)$ or $S_\nu(S_\pi)=1(0)$; and $S=0,1,2$ corresponds to $S_\pi=S_\nu=1$. From the reduction rule of SU(3)→SO(3) [7] it is easy to obtain the orbital angular momentum **L**. The total angular momentum is determined by $\mathbf{J}=\mathbf{L}+\mathbf{S}$. In $k(\lambda,\mu)^S_{\pi\nu}$, k denotes the number of times that the irreducible representation $(\lambda,\mu)^S_{\pi\nu}$ appears. k is omitted for the sake of simplicity in the case of $k=1$.

N_π	N_ν	$(\lambda_\pi,\mu_\pi)^{S_\pi}$	$(\lambda_\nu,\lambda_\nu)^{S_\nu}$	$(\lambda,\mu)^S_{\pi\nu}$
			sd shell	
1	1	$(4,0)^0$, $(2,1)^1$	$(4,0)^0$, $(2,1)^1$	$(8,0)^0$, $(6,1)^0$, $2(6,1)^1$
1	2	$(4,0)^0$, $(2,1)^1$	$(4,2)^0$, $(5,0)^1$	$(8,2)^0$, $(6,3)^0$, $(6,3)^1$, $(9,0)^1$, $(7,1)^{0,1,2}$
1	3	$(4,0)^0$, $(2,1)^1$	$(6,0)^0$, $(3,3)^1$, $(4,1)^1$	$(10,0)^0$, $(8,1)^0$, $2(8,1)^1$, $(7,3)^1$
2	2	$(4,2)^0$, $(5,0)^1$	$(4,2)^0$, $(5,0)^1$	$(8,4)^0$, $(6,5)^0$, $2(9,2)^1$, $(10,0)^{0,1,2}$
2	3	$(4,2)^0$, $(5,0)^1$	$(6,0)^0$, $(3,3)^1$, $(4,1)^1$	$(10,2)^0$, $(8,3)^0$, $(11,0)^1$, $(9,1)^{0,1,2}$ $(7,5)^1$, $2(8,3)^1$, $(8,3)^{0,1,2}$
3	3	$(6,0)^0$, $(0,6)^0$, $(3,3)^{0,1}$	$(6,0)^0$, $(0,6)^0$, $(3,3)^{0,1}$	$(12,0)^0$, $(0,12)^0$, $(10,1)^0$, $2(9,3)^{0,1}$, $2(3,9)^{0,1}$
			pf shell	
1	1	$(6,0)^0$, $(4,1)^1$	$(6,0)^0$, $(4,1)^1$	$(12,0)^0$, $(10,1)^0$, $2(10,1)^1$
1	2	$(6,0)^0$, $(4,1)^1$	$(8,2)^0$, $(9,0)^1$	$(14,2)^0$, $(12,3)^0$, $(12,3)^1$, $(15,0)^1$, $(13,1)^1$, $(13,1)^{0,1,2}$
1	3	$(6,0)^0$, $(4,1)^1$	$(12,0)^0$, $(6,6)^0$, $(9,3)^1$, $(10,1)^1$	$(18,0)^0$, $(16,1)^0$, $(12,6)^1$, $(15,3)^1$, $2(16,1)^1$, $(10,7)^1$, $(13,4)^{0,1,2}$, $(14,2)^{0,1,2}$,
1	4	$(6,0)^0$,$(4,1)^1$	$(10,4)^0$, $(11,2)^1$	$(16,4)^0$, $(14,5)^0$, $(14,5)^1$, $(17,2)^1$, $(15,3)^{0,1,2}$
2	2	$(8,2)^0$, $(9,0)^1$	$(8,2)^0$, $(9,0)^1$	$(16,4)^0$, $(14,5)^0$, $2(17,2)^1$, $(18,0)^{0,1,2}$,
2	3	$(8,2)^0$, $(9,0)^1$	$(12,0)^0$, $(6,6)^0$, $(9,3)^1$, $(10,1)^1$	$(20,2)^0$, $(14,8)^0$, $(18,3)^0$, $(21,0)^1$, $(19,1)^1$, $(15,6)^1$, $(18,3)^{0,1,2}$, $(19,1)^{0,1,2}$
2	4	$(8,2)^0$, $(9,0)^1$	$(10,4)^0$, $(11,2)^1$	$(18,6)^0$, $(16,7)^0$, $2(19,4)^1$, $(20,3)^{0,1,2}$
3	3	$(12,0)^0$, $(6,6)^0$ $(9,3)^1$, $(10,1)^1$	$(12,0)^0$, $(6,6)^0$ $(9,3)^1$, $(10,1)^1$	$(24,0)^0$, $(22,1)^0$, $(12,12)^0$, $2(21,3)^1$, $2(22,1)^1$, $2(15,9)^1$, $2(16,7)^1$, $(18,6)^{0,1,2}$
3	4	$(12,0)^0$, $(6,6)^0$, $(9,3)^1$, $(10,1)^1$	$(10,4)^0$, $(11,2)^1$	$(22,4)^0$, $(20,5)^0$, $(16,10)^0$, $(14,11)^0$, $(19,7)^1$ $(20,5)^1$, $(23,2)^1$, $(21,3)^1$, $(21,3)^{0,1,2}$, $(20,5)^{0,1,2}$
4	4	$(10,4)^0$, $(11,2)^1$	$(10,4)^0$, $(11,2)^1$	$(20,8)^0$, $(18,9)^0$, $2(21,6)^1$,$2(19,7)^1$, $(22,4)^{0,1,2}$
			sdg shell	
1	1	$(8,0)^0$, $(6,1)^1$	$(8,0)^0$, $(6,1)^1$	$(16,0)^0$, $(14,1)^0$, $2(14,1)^1$, $2(12,2)^1$, $(12,2)^{0,1,2}$
1	2	$(8,0)^0$, $(6,1)^1$	$(12,2)^0$, $(13,0)^1$	$(20,2)^0$, $(18,3)^0$, $(18,3)^1$, $(21,0)^1$, $(19,1)^{0,1,2}$
1	3	$(8,0)^0$, $(6,1)^1$	$(18,0)^0$, $(15,3)^0$, $(15,3)^1$	$(26,0)^0$, $(24,1)^0$, $(23,3)^0$, $(23,3)^1$, $(24,1)^1$, $(21,4)^1$, $(21,4)^{0,1,2}$
1	4	$(8,0)^0$, $(6,1)^1$	$(18,4)^0$, $(20,0)^0$, $(19,2)^1$	$(26,4)^0$, $(24,5)^0$, $(28,0)^0$, $(27,2)^1$, $(24,5)^1$, $(26,1)^1$
2	2	$(12,2)^0$, $(13,0)^1$	$(12,2)^0$, $(13,0)^1$	$(24,4)^0$, $(22,5)^0$, $2(25,2)^1$, $(26,0)^{0,1,2}$,
2	3	$(12,2)^0$, $(13,0)^1$	$(18,0)^0$, $(15,3)^0$, $(15,3)^1$	$(30,2)^0$, $2(28,3)^0$, $(27,5)^0$, $(27,5)^1$, $2(28,3)^1$, $(31,0)^1$, $(28,3)^{0,1,2}$
2	4	$(12,2)^0$, $(13,0)^1$	$(18,4)^0$, $(20,0)^0$, $(19,2)^1$	$(30,6)^0$, $(28,7)^0$, $(32,2)^0$, $(30,3)^0$, $(31,4)^1$, $(33,0)^1$, $(31,4)^1$, $(32,2)^{0,1,2}$
3	3	$(18,0)^0$, $(15,3)^0$, $(15,3)^1$, $(16,1)^1$	$(18,0)^0$, $(15,3)^0$, $(15,3)^1$, $(16,1)^1$	$(36,0)^0$,$2(33,3)^0$, $(34,1)^0$, $(30,6)^0$, $2(33,3)^1$, $2(30,6)^1$, $2(34,1)^1$, $(30,6)^{0,1,2}$
3	4	$(18,0)^0$, $(15,3)^0$, $(15,3)^1$	$(18,4)^0$, $(20,0)^0$, $(19,2)^1$	$(36,4)^0$, $(34,5)^0$, $(33,7)^0$, $(38,0)^0$, $(35,3)^0$, $(33,7)^1$, $(35,3)^1$, $(37,2)^1$, $(34,5)^1$, $(34,5)^{0,1,2}$
4	4	$(18,4)^0$, $(20,0)^0$, $(19,2)^1$	$(18,4)^0$, $(20,0)^0$, $(19,2)^1$	$(36,8)^0$, $2(38,4)^0$, $(40,0)^0$, $2(37,6)^1$, $2(39,2)^1$, $(38,4)^{0,1,2}$

TABLE IV. Comparison of binding energies ($N_\pi = N_\nu = 3$) for *sd*, *pf*, and *sdg* shells. The unit is MeV.

	sd shell	*pf* shell	*sdg* shell
Exact shell model	720	2592	5616
SD truncation	720	1946	3688

$$y(aa0) = \hat{a}\frac{v_a}{u_a} = \hat{a}\sqrt{\left(\frac{N}{\Omega - N}\right)^{1/2}}, \tag{9}$$

and the D pair is obtained by using the commutator [8]

$$D^\dagger = \frac{1}{2}[Q, S^\dagger] = \sum_{ab} y(ab2)(C_a^\dagger \times C_b^\dagger)^2. \tag{10}$$

Here the operator Q is defined in Eq. (5). From Eq. (10), it is easy to obtain

$$y(ab2) = -q(ab)\sqrt{\left(\frac{N}{\Omega - N}\right)^{1/2}}, \tag{11}$$

There are other ways to define D pair, but it is expected that the above way is one of the best ways when the quadrupole-quadrupole interaction between protons and neutrons are strong. For nuclei with proton numbers and/or neutron numbers near the magic number(s) where interactions between like particles are important compared with those between unlike particles, we must seek other methods. Note that we have omitted the subscript σ in Eqs. (9)–(11) since we determine the *SD* pairs separately for protons and neutrons in the same way, and this omission does not cause confusion.

Within the subspace made of the above *SD* pairs, Hamiltonian (7) is diagonalized to calculate the binding energies, the excited levels, wave functions, and $E2$ transition rates. Table IV lists a comparison between binding energies calculated in the full SM space [here we use analytical formulas of the Elliott's SU(3) model], and those calculated within the framework of the *SD* nucleon pair shell model. We see that the binding energies calculated in the *SD*-pair subspace in all cases (except $N_\pi = N_\nu = 3$ in the *sd* shell, where they are the same) are much smaller than those calculated in the full SM space. It is consistent with the above single j case where the contribution to the binding energy from the quadrupole-quadrupole interaction in the *SD* subspace is smaller than that in the shell model space. This difference seems to become larger and larger with the major quantum n of the shell, or the number of single-particle levels. It is easy to note in Table III that there are two degenerate''ground'' bands for the $N_\pi = N_\nu = 3$ case of the *sd* shell; they belong to the $(\lambda,\mu)_{\pi\nu} = (12,0)^0_{\pi\nu}$ and $(0,12)^0_{\pi\nu}$ cases, respectively. For the sake of simplicity, however, we refer to a band which corresponds to a $(12,0)^0_{\pi\nu}$ irreducible representation as the ground band in the following discussion of this paper for the $N_\pi = N_\nu = 3$ case of the *sd* shell. The states corresponding to a $(0,12)^0_{\pi\nu}$ irreducible representation are not reproduced in the above *SD*-pair subspace, but it can be exactly reproduced within the *SDG*-pair subspace.

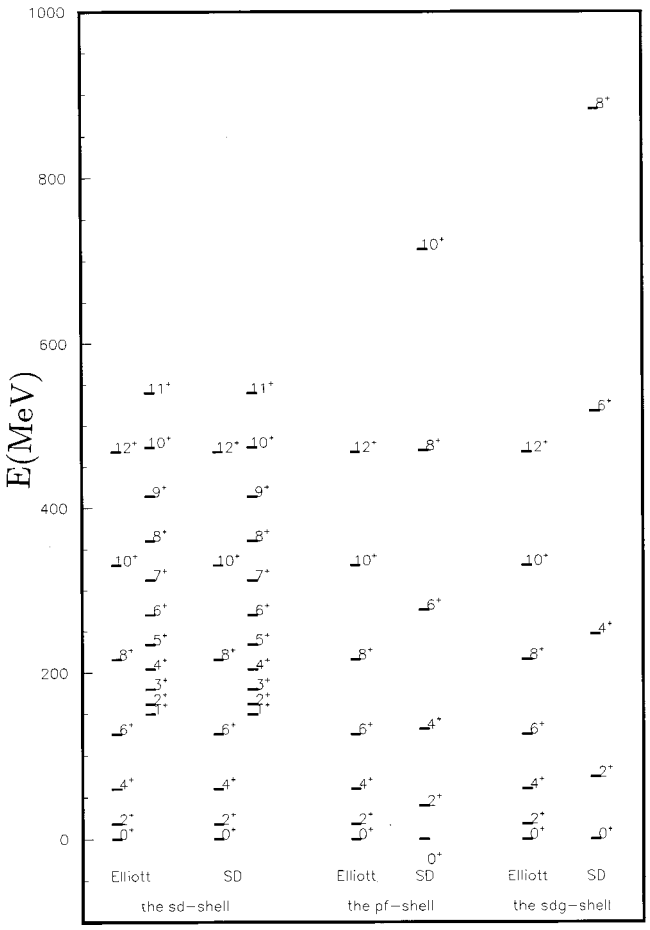

FIG. 3. Excitation energies in the ($N_\pi = N_\nu = 3$) *sd*, *pf*, and *sdg* shells. ''Elliot'' means results of the Elliott model, and ''*SD*'' means results using the *SD*-pair truncation. In the *sd* shell the two lowest-lying bands are listed and compared (the corresponding energies are equal to each other within a numerical error). The ground bands calculated using the Elliott model are compared with those calculated using the *SD*-pair truncation for the *pf* and *sdg* shells. Note that the ground band which corresponds to the SU(3) irreducible representation of the *sd* shell, $(\lambda,\mu)^S_{\pi\nu} = (0,12)^0_{\pi\nu}$, is omitted for the sake of simplicity.

Figure 3 presents the excited energies calculated in the *SD*-pair subspace, and those calculated within the framework of the Elliott model. From Table IV and Fig. 3, we see that in the *sd* shell, the calculation of the *SD* truncation reproduces exact Elliott model results for the two lowest bands when $N_\pi = N_\nu = 3$. We mention without presentation of further details that all states of irreducible representations in the Elliott model, $(12,0)^0_{\pi\nu} + (10,1)^0_{\pi\nu} + (8,2)^0_{\pi\nu} + (6,3)^0_{\pi\nu} + (4,4)^0_{\pi\nu} + (2,5)^0_{\pi\nu} + (0,6)^0_{\pi\nu} = (6,0)^0_\pi \times (6,0)^0_\nu$, are reproduced in the *SD*-pair subspace with a precision of eight effective digits. This means that all states in the lowest band for the single-closed *sd* shell ($N = 3$ case), which correspond to the irreducible representation (6,0), are fully taken into account in the above *SD*-pair subspace, and the behavior of the neutron-proton coupling term $Q_\pi \cdot Q_\nu$ in the *SD*-pair subspace is the *same* as that in the full shell model space. It is an interesting question in mathematics to know why low-lying bands in the

TABLE V. $E2$ transition strengths (*sd*, *pf*, and *sdg* shell) in the *SD*-pair subspace for $N_\pi = N_\nu = 3$. We use $e_\pi = 1.6e$ and $e_\nu = 1.6e$. The unit of the $E2$ transition strengths is e^2 fm^2. In the first column of each shell we list the $E2$ transition rates calculated in the *SD*-pair subspace. The exact $E2$ transition rates calculated in the Elliott model are listed in the second column of each shell case. The $E2$ transition rates (in percentage) relative to $B(E2, 2_1^+ \to 0_1^+)$ are listed in the third column, where the first half of the data corresponds to the *SD* subspace, and the data after the / correspond to the analytical results of the Elliott model. In the *sd* shell some $E2$ transition rates are exactly reproduced.

	sd shell			*pf* shell			*sdg* shell		
$2_1^+ \to 0_1^+$	368.6	368.6	100/100	873.3	1327.1	100/100	1641.2	2875.4	100/100
$4_1^+ \to 2_1^+$	497.4	497.4	134.9/134.9	1174.6	1866.5	134.5/134.9	2208.7	4078.4	134.6/141.2
$6_1^+ \to 4_1^+$	489.8	489.8	132.9/132.9	1150.6	1997.9	131.8/132.9	2165.5	4434.0	131.9/154.2
$8_1^+ \to 6_1^+$	425.0	425.0	115.3/115.3	991.5	2003.7	113.5/151.0	1867.5	4553.8	113.8/158.4
$10_1^+ \to 8_1^+$	318.7	318.7	86.5/86.5	737.6	1940.2	84.5/146.8	1389.7	4559.5	84.7/158.6
$12_1^+ \to 10_1^+$	176.3	176.3	47.8/47.8	404.3	1826.5	46.3/138.3	761.7	4370.0	46.4/156.2
$4_1^+ \to 2_2^+$	<0.1	0	-	<0.1	0	-	<0.1	0	-
$2_2^+ \to 0_1^+$	<0.1	0	-	<0.1	0	-	<0.1	0	-
$2_2^+ \to 2_1^+$	<0.1	0	-	<0.1	0	-	<0.1	0	-
$6_2^+ \to 4_1^+$	<0.1	0	-	<0.1	0	-	<0.1	0	-

case of an *sd* shell with six particles, which is a half-filled case, are exactly reproduced, although we diagonalize the Hamiltonian in a smaller configuration space. Up to now we do not know whether this exact reproduction is accidental, or whether there are deep reasons lying behind it. For *pf* and *sdg* shells, the agreement for $N_\pi = N_\nu = 3$ (which is not a half-filled case) does not become so good. For example, our result is just 66% of the total binding energy in the Elliott model when $N_\pi = N_\nu = 3$ in the *sdg* shell. It is then worth trying to see whether, in general, one obtains the analytical results of the Elliott model using the above *SD*-pair truncation in the half-filled shell. For the *sdg* shell, $N_{\max} = 7$ is *not* a half-filled case like the above, and we can skip it. $N_{\max} = 5$ for the *pf* shell is the only candidate to check the above ansatz, because the $N_{\max}$ of the next shell ($n = 11$) which satisfies the above half-filled condition is 33. However, calculations of $N = 5$ are so time consuming that one must modify the code using some novel techniques [9,10].

In Table V we present a comparison between the $E2$ transition rates calculated in the *SD*-pair subspace and those calculated using the analytical formulas of the Elliott model for each shell case. In order to see the physics more clearly, we list the $E2$ transition rates relative to $B(E2, 0_1^+ \to 2_1^+)$. It is easy to note that we have numerically reproduced the $E2$ transition rates between states of the ground band for the *sd* shell case, and the $E2$ transition rates calculated in the *SD*-pair subspace are systematically smaller than the exact results calculated in the full SM space for the *pf* and *sdg* shells. However, the relative $E2$ transition rates are reasonably reproduced for the lowest excitations ($J \leqslant 6$). For the case of $J \geqslant 8$ one needs coherent G pairs. Although there are such differences, basic properties such as the band structure are kept very well. In the calculation of the *SD*-pair approximation the $E2$ transition rates from the other bands to the ground band are seven orders smaller than the strengths between the ground band states. It is also interesting to note that the relative $E2$ transition rates calculated in the *SD*-pair subspace are almost the same from the *sd* shell to the *sdg* shell, while those calculated in the full SM space change quickly for higher J states.

Another difference between *SD* truncation and the full shell model is very parent in Fig. 3. The calculated energy levels (moment of inertia) in the *SD* configuration are systematically higher (smaller), and binding energies are smaller than the full shell model (Elliott model) results. However, all the calculated intervals and the sequences within each column of Fig. 3, and the transition probabilities between the states, exhibit definite band regularities of rotational nuclei. This phenomenon was observed in the two-*j* single-closed shell in previous papers, such as Ref. [4]. This is very important since the *SD* truncation does not lose the essential physics of the shell model. In particular the differences in the moments of inertia and binding energies can be easily eliminated using different parametrizations. To show this point, we present a typical example in Fig. 4, where we use 24.2% of the original value κ to obtain a best fit with the original Elliott model for the ground band. We see that the agreement of the ground band is satisfactory. The difference is that the band heads of the *SD* truncation are much lower than those in the Elliott model. Here we have omitted the details of the $E2$ transitions for the states in Fig. 4, because there would be too many data in a table (note that the $E2$ transition results remain untouched when we change κ. Thus one can refer to Table V for the two lowest bands), but we would like to present a description of the $E2$ transitions calculated using the *SD*-pair approximation. The intraband $E2$ transitions are much stronger than the interband $E2$ transitions (at least ten times), except in one case which will be discussed below. This is a property of band structures in well-deformed nuclei. Another interesting point is that these levels within the band satisfactorily follow the rule of $L(L+1)$ as the Elliott model, and moments of inertia remain to be slightly changed for all bands. There are several ''identical bands'' which can be regarded as an image of the fact

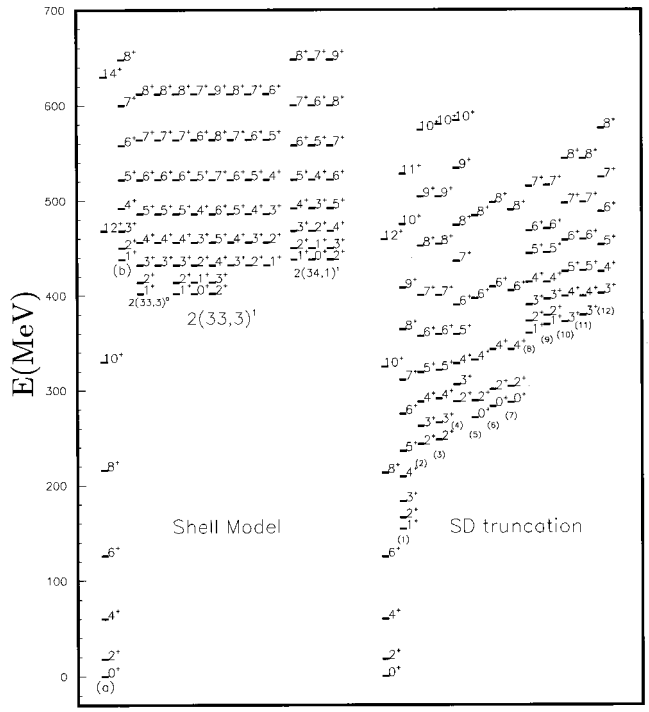

FIG. 4. Excitation levels in the $(N_\pi = N_\nu = 3)$ *sdg* shell. The unit of energy is in MeV. Here higher states in the shell model (Elliott model) are omitted because they cannot exist in the *SD* subspace. On the left-hand side, the Elliott notations of the $SU(3)_{\pi\nu}$ group are given below the corresponding band heads. The number ''2'' before the bra of some irreducible representations denotes that the corresponding representations appear twice. Here, due to the limitation of space, we have omitted repetitions of energy levels which correspond to the same irreducible representation. (a) and (b) correspond to the SU(3) irreducible representations $(36,0)^0$ and $(34,1)^0$, respectively. The right-hand side lists calculational results using the *SD*-pair truncation, where sequences of the bands are labeled below the corresponding bandheads. The parameter κ is chosen to be 24.2% of the original value on the right-hand side.

that one irreducible representation may appear many times. On the right-hand side of Fig. 4, bands (2) and (3) can be regarded as one example that one irreducible representation appears twice. In this case, both the energy levels and $E2$ transitions are almost the same without any exception. The other three examples are bands (6) and (7) (twice), bands (8) and (9) (twice), and bands (10) and (11). Bands (4) and (5) belong to another case. These two bands can be regarded as sequences of irreducible representation $(\lambda,2)$. The states 2^+, 4^+, etc., within bands (4) and (5) are almost identical, and there are non-negligible $E2$ transitions between interband states as well as very strong $E2$ transitions between intraband states. The calculated transition rates between intraband states are usually two or more times larger than those between interband states. In this example 100 calculated states are presented, and the lowest 60 states are exhausted in the *SD* subspace. This means that the above discussion is not special but rather general. Although we are unable to reproduce all the corresponding bands of the Elliott model using the *SD* truncation, the results in Fig. 4 clearly demonstrate that essential properties of the Elliott model are well reproduced. This is important since it means that the *SD* truncation can be a good approximation of the shell model for rotational motion (after adjusting parameters).

V. DISCUSSION AND CONCLUSION

In this paper, we carry out schematic calculations within the shell model space and collective *SD*-pair subspace. A comparison between calculations in the full shell model space and in the *SD*-pair subspace is presented and discussed. In the single-*j* case, when the Hamiltonian consists of monopole and quadrupole pairing plus quadrupole pairing the *SD*-pair subspace satisfactorily reproduces the low-lying levels of the shell model and the $E2$ transitions between them. The contributions from the monopole pairing and quadrupole-quadrupole interaction are the reverse, and as a consequence of this offset the total binding energies calculated in the *SD*-pair subspace agree well with results calculated in the full shell model space. The *SD*-pair truncation deteriorates if the quadrupole-quadrupole interaction is artificially large compared with the monopole pairing interaction. On the other hand, the larger monopole pairing strength does not deteriorate the agreement between the *SD*-pair truncation and the SM space. When the neutron pair number is greater than 3 and $N_\pi = 1$ or 2, among the contribution from every term of the Hamiltonian there are quite large differences between the results calculated in the SM space and those calculated in the *SD*-pair subspace for the monopole pairing term and quadrupole-quadrupole interaction. The differences between the above two kinds of calculations for these two terms are comparable in magnitude and opposite in sign. These differences become very small for the cases of $N_\pi = 3$ or $N_\nu = 3$. Because we use a moderate pairing strength and a quadrupole-quadrupole interaction for this small single-*j* shell, the agreement of the binding energy between the calculation in the full SM space and that in the *SD*-pair subspace is extremely good in this paper. The agreement of energy levels and the $E2$ transitions between low-lying states are also good. This means that the *SD*-pair truncation for a single-*j* shell is reasonable when the Hamiltonian consists of pairing and quadrupole-quadrupole interaction. In the multi-*j* case, we assume the Hamiltonian is of pure quadrupole-quadrupole type, and that the single-particle levels are determined to be of three-dimensional harmonic vibrator type. In the half-filled case of the *sd* shell, the exact reproduction of some states within the *SD*-pair subspace is unexpected, and needs further investigation. From the calculation, we find that although the *SD*-pair subspace is much smaller than the original shell model space, essential properties such as the band structure within the shell model space survive in the *SD*-pair subspace. The differences in moments of inertia or binding energies can be easily eliminated using different parameters. Note that it seems impossible to fit the moments of inertia and binding energies at the same time by adjusting κ in the above *pf* and *sdg* shells, because one should use a smaller κ to fit the excited energies (cf. larger κ to fit the binding energies). The difficulty can be overcome by introducing $\vec{L}^2$ interaction in the Elliott model, and in that

case we can fit both moments of inertia and binding energies using two different parameters. Despite the differences in parameters, essential properties of the Elliott model are kept intact in the *SD*-pair truncation, because the introduction of $\vec{L}^2$ does not cause any changes in the wave functions and $B(E2)$ transitions. Therefore, it would be interesting to apply the *SD*-pair truncation to realistic nuclei, and see how well the *SD*-pair truncation works. Recently, the O(6) properties of doubly even nuclei in the $A\sim 130$ region have been successfully reproduced within the *SD*-pair subspace [9]. This can be regarded as a verification of the *SD*-pair truncation of the shell model in realistic cases.

ACKNOWLEDGMENTS

We would like to thank Professor Stuart Pittel and Professor V. K. B. Kota for valuable discussions and kind assistance. One of the authors (Y.M.Z.) gratefully acknowledges the Science and Technology Agency of Japan (Contract No. 297040) for supporting this project.

[1] A. Arima and F. Iachello, Ann. Phys. (N.Y.) **99**, 253 (1976); **111**, 201 (1978); **123**, 468 (1979). For a review, see F. Iachello and A. Arima, *The Interacting Boson Model* (Cambridge University, Cambridge, 1987).

[2] J. Q. Chen, B. Q. Chen, and A. Klein, Nucl. Phys. **A554**, 61 (1993); **A562**, 218 (1993).

[3] J. Q. Chen, Nucl. Phys. **A626**, 686 (1997).

[4] N. Yoshinaga, T. Mizusaki, A. Arima, and Y. D. Devy, Prog. Theor. Phys. Suppl. **125**, 65 (1996), and references therein.

[5] S. Yoshida, Phys. Rev. **123**, 2122 (1961).

[6] B. Q. Chen (unpublished); Y. M. Zhao, Ph.D. thesis, Nanjing University, 1995; Y. M. Zhao and J. Q. Chen, High Energy Phys. Nucl. Phys. **21**, 356 (1997).

[7] J. P. Elliott, Proc. R. Soc. London, Ser. A **245**, 128 (1958); M. Harvey, Adv. Nucl. Phys. **1**, 67 (1968); K. Brahmam and R. Raju, At. Data Nucl. Data Tables **16**, 166 (1975).

[8] K. Allart, E. Boeker, G. Bonsignori, M. Saroia, and Y. K. Gambhir, Phys. Rep. **169**, 209 (1988); I. Talmi, Nucl. Phys. **A172**, 1 (1972).

[9] Y. M. Zhao, S. Yamaji, N. Yoshinaga, and A. Arima, Phys. Rev. C **62**, 014315 (2000), preceding paper.

[10] Y. M. Zhao, N. Yoshinaga, S. Yamaji, J. Q. Chen, and A. Arima, Phys. Rev. C **62**, 014304 (2000), this issue.